Atmos. Chem. Phys. Discuss., 12, 2131–2166, 2012
www.atmos-chem-phys-discuss.net/12/2131/2012/
doi:10.5194/acpd-12-2131-2012

Atmospheric Chemistry and Physics Discussions

An assessment of atmospheric mercury in the Community Multiscale Air Quality (CMAQ) model

T. Holloway[1], C. Voigt[1], J. Morton[1], S. N. Spak[2], A. P. Rutter[3], and J. J. Schauer[4]

[1]Nelson Institute Center for Sustainability and the Global Environment (SAGE), University of Wisconsin-Madison, Madison, WI, USA
[2]Public Policy Center (PPC), University of Iowa, Iowa City, IA, USA
[3]Civil and Environmental Engineering, Rice University, Houston, TX, USA
[4]Civil and Environmental Engineering, University of Wisconsin-Madison, Madison, WI, USA

Received: 15 December 2011 – Accepted: 22 December 2011 – Published: 23 January 2012

Correspondence to: T. Holloway (taholloway@wisc.edu)

Published by Copernicus Publications on behalf of the European Geosciences Union.

Abstract

Quantitative analysis of three atmospheric mercury species – gaseous elemental mercury (Hg^0), reactive gaseous mercury (RGHg) and particulate mercury (PHg) – has been limited to date by lack of ambient measurement data as well as by uncertainties in numerical models and emission inventories. This study employs the Community Multiscale Air Quality Model version 4.6 with mercury chemistry (CMAQ-Hg), to examine how local emissions, meteorology, atmospheric chemistry, and deposition affect mercury concentration and deposition the Great Lakes Region (GLR), and two sites in Wisconsin in particular: the rural Devil's Lake site and the urban Milwaukee site. Ambient mercury exhibits significant biases at both sites. Hg^0 is too low in CMAQ-Hg, with the model showing a 6 % low bias at the rural site and 36 % low bias at the urban site. Reactive mercury (RHg = RGHg + PHg) is over-predicted by the model, with annual average biases >250 %. Performance metrics for RHg are much worse than for mercury wet deposition, ozone (O_3), nitrogen dioxide (NO_2), or sulfur dioxide (SO_2). Sensitivity simulations to isolate background inflow from regional emissions suggests that oxidation of imported Hg^0 dominates model estimates of RHg at the rural study site (91 % of base case value), and contributes 55 % to the RHg at the urban site (local emissions contribute 45 %). Limited evidence on the lifetime of RHg transported to the rural site suggests that modeled dry deposition rates are too high, possibly compensating for the erroneously high RHg values.

1 Introduction

Although only <5 % of global mercury resides in reactive form, this fraction is subject to more rapid chemical reactions and faster deposition to the Earth surface (Lindberg et al., 2007). Reactive mercury species (RHg) are considered to be the sum of reactive gaseous mercury (RGHg) and particulate mercury (PHg), with atmospheric lifetimes ranging from a few days to weeks (Selin, 2009). The majority of mercury in the

ACPD
12, 2131–2166, 2012

atmosphere exists as elemental mercury (Hg^0), which has been shown to be a major source of RHg, (Lin and Pehkonen, 1999). However atmospheric models differ in the attribution of dominant chemical pathway for oxidation of Hg^0 to RHg and many components of the mercury budget remain uncertain.

This study evaluates the skill of a widely used regional chemical transport model for studying mercury, the Community Multiscale Air Quality (CMAQ) model, developed by the US Environmental Protection Agency (EPA) and directly used in mercury policy development (Bullock and Braverman, 2007). Here, we focus on CMAQ v. 4.6 including mercury chemistry, hereafter referred to as CMAQ-Hg.

For the most part, model performance in simulating mercury over North America has been evaluated against wet deposition measured in the US by the EPA Mercury Deposition Network (MDN). A number of studies have used these data to evaluate CMAQ-Hg (Bash, 2010; Bullock and Brehme, 2002; Bullock et al., 2009; Gbor et al., 2006, 2007; Lin et al., 2007; Lin and Tao, 2003; Vijayaraghavan et al., 2007), and other atmospheric chemistry models that include mercury (Cohen et al., 2004; Holmes et al., 2010; Sanei et al., 2010; Seigneur et al., 2003a; Selin and Jacob, 2008; Vijayaraghavan et al., 2008). Most studies that evaluate model estimates of ambient mercury compare with Total Gaseous Mercury (TGM) and/or Hg^0 (Gbor et al., 2006, 2007; Holmes et al., 2010; Lin and Tao, 2003; Lohman et al., 2008; Selin et al., 2007; Soerensen et al., 2010; Wen et al., 2011). These measurements have supported model development, but they do not allow for a detailed evaluation of model chemical processes.

Global and regional atmospheric chemistry models have been compared with ambient, speciated mercury measurements in a few studies, typically over periods of a month or less. Aircraft measurements over a 12-day period in June 2000 found that CMAQ-Hg overestimated RGHg near the surface, but underestimated concentrations aloft (Sillman et al., 2007). Over Asia RHg simulated by CMAQ-Hg was too high at all sites, whereas Hg^0 was under-predicted at urban sites (Lin et al., 2010). When annual average RGHg values were compared between the global GEOS-Chem model and observations, the model values exceeded observations at 10 of the 13 sites

ACPD
12, 2131–2166, 2012

compared, averaged nearly 50 % higher (model average: 20.08 pg m^{-3}; observation average: 13.58 pg m^{-3}), and showed much less spatial variability (standard deviation of model values: 1.78 pg m^{-3}; standard deviation of observed means: 8.02 pg m^{-3}) (Selin et al., 2007). The global CTM-Hg also has been shown to calculate RGHg values exceeding observations by over a factor of four (Seigneur et al., 2004). The tendency of models to over-predict RGHg also appears in the ROME plume model (Lohman et al., 2006). This consistent over-prediction of reactive mercury suggests that fundamental processes are not well captured by existing models, and that adequate simulation of wet deposition (dominated by RHg) may be due to compensating errors in deposition or other chemical processes.

Here we explore the ability of CMAQ-Hg to capture Hg^0, RGHg and PHg at both rural and urban locations, over a nearly full year of measurements. We devote attention to two sites: rural Devil's Lake, Wisconsin (Manolopoulos et al., 2007), and urban Milwaukee, Wisconsin. By comparing model performance at these two sites, we evaluate model chemical processes, emissions, and deposition.

2 Model and observations

Discussion focuses on the two measurement sites: Devil's Lake (DL, located at 43.43° N, 89.68° W) and Milwaukee (MKE, located at 43.12° N, 87.88° W), shown in Fig. 1. The measurements were gathered for just under a full year at both sites; DL from 10 April 2003 to 19 March 2004, MKE from the 29 June 2004 to 13 May 2005. Because air quality at MKE is heavily influenced by local emissions, the DL site was considered to better reflect model processes. Thus, the model simulation was conducted for the full year of 2003 to allow for comparison with the DL observations. As discussed below, CMAQ-Hg results diverge significantly from DL and MKE values, even on a monthly mean basis, suggesting that inconsistencies with MKE cannot be attributed to meteorology in any significant way. Thus, model simulations were limited to 2003 for comparison with both sites.

ACPD
12, 2131–2166, 2012

2.1 Overview of CMAQ-Hg model

We employed CMAQ-Hg version 4.6 (Bullock and Braverman, 2007; Byun and Schere, 2006), using a horizontal resolution of 36 km × 36 km simulations for the Continental US (CONUS) domain and a horizontal resolution of 12 km × 12 km for the Great Lakes Region (GLR) domain, shown in Fig. 1. Both simulations used 15 model layers in the vertical with an average model top of 16 km altitude and a average surface layer thickness of 50 m. CMAQ-Hg was run using the default boundary conditions (Table A1) for CONUS simulations, and the CONUS model output was used to provide hourly boundary conditions for simulations over the GLR.

The model was configured to use the Carbon Bond Five (CB05) lumped gas phase chemistry mechanism (Sarwar et al., 2008) the AERO4 aerosol mechanism (Binkowski and Roselle, 2003), the global mass-conserving Yamartino advection scheme, and the Asymmetrical Convective Model with mercury (ACM2), which controls cloud formation, vertical diffusion, and eddy diffusion. This version of CMAQ-Hg builds on earlier releases of CMAQ-Hg (Bullock and Brehme, 2002). The CB05 mechanism with mercury is the only gas phase chemistry module in CMAQ to include mercury chemistry and, since it was developed for the regional scale (Gery et al., 1989), the mechanism is well suited for our focus on the GLR. The core mechanism includes 56 chemical species (52 core species and 4 mercury species), 156 non-mercury gas-phase reactions, 4 gas-phase reactions involve mercury, 6 aqueous reactions involving mercury and 7 sorption/de-sorption mercury reactions. CMAQ-Hg 4.6 reports modal bulk oxidized mercury species (RGM and PHg) using the operationally defined nomenclature for compounds collected and measured (Lu et al., 1998; Landis et al., 2002). Internally, CMAQ-Hg 4.6 follows the gas-phase and aqueous-phase chemistry of mercury using the true chemical species, such as HgO and $HgCl_2$ (for a full details of chemical reactions and speciation see Bullock and Brehme, 2002; Lin et al., 2007) and then converts these species to RGM and PHg whenever they are present in either the gas phase or in modal aerosol particles which have not been activated into cloud droplets. Aqueous mercury chemistry considers activated accumulation mode aerosols.

ACPD
12, 2131–2166, 2012

Dry deposition is calculated in CMAQ-Hg in the meteorology preprocessor, MCIP v. 3.4 with the M3DRY scheme, which explicitly treats Hg^0 and RGHg dry deposition based on the amount of vegetation cover, vegetation type and stomatal resistance (Lin et al., 2006; Pleim et al., 1999). Dry deposition of PHg is governed by the aerosol scheme AERO4, and is a function of particle size, always treated as either Aitken or accumulation mode (Binkowski and Shankar, 1995). Wet deposition of Hg^0 and RGHg is calculated in a manner analogous to all other species with aqueous chemistry, and depends on cloud water concentration along with the rate of precipitation during the cloud's lifetime. For particulates, including PHg, wet deposition depends on the particle size. Due to the different treatment of accumulation and coarse mode than Aitken mode particles, any modeled precipitation will deposit all accumulation-mode PHg, but Aitken-mode PHg may remain in the atmosphere if the cloud lifetime is not sufficiently long.

The Advanced Research Weather Forecasting Model (ARW-WRF) version 3.0, referred to here as WRF (Skamarock and Klemp, 2008), was used to generate continuous meteorology over the study regions, constrained with assimilated data from the 2003 North American Regional Reanalysis (NARR) dataset (Mesinger et al., 2006). The simulation compares well with NARR for temperature and precipitation over the CONUS and GLR domains.

All emissions are taken from the 2002 EPA National Emissions Inventory (NEI), and prepared for use in CMAQ with the Sparse Matrix Operator Kernel Emissions Model version 2.4 (SMOKE). At the time the study began, the 2002 NEI was the most up-to-date inventory of US emissions, and includes Canadian and Mexican sources.

Over the GLR, electric-generating units (EGUs) are the largest source of mercury emissions at 55 %, a higher fraction than the CONUS average EGU contribution of 43 %. The highest total emissions, for both the CONUS and GLR domains, are clustered around coal-fired power plants along the Ohio River and western Pennsylvania, where local coal is high in mercury (Toole-O'Neil et al., 1999), and over larger cities. Spatial patterns in speciation of emissions, shown in Fig. A1, such as the abrupt shifts

ACPD
12, 2131–2166, 2012

in percentage Hg^0 and RGHg contribution at the US-Canada border and certain state borders (e.g. Illinois-Wisconsin), are likely due to differences in data collection and organizational methods.

2.2 Ambient air quality measurements from EPA AQS

To compare CMAQ-Hg results with more widely studied pollutants, observations for ozone (O_3), nitrogen dioxide (NO_2), and sulfur dioxide (SO_2) were obtained from the US EPA Air Quality System database (http://www.epa.gov/ttn/airs/aqsdatamart/). The AQS database contains measurements of criteria and hazardous air pollutants across the United States, going back over ten years. Daily average observations from January and July 2003, taken at DL and MKE when available, were compared with daily average values from the lowest model layer of CMAQ-Hg in the corresponding grid cell. For DL, there was only one AQS monitor in proximity (WI site #7). For the MKE location, there were several AQS monitors within close proximity to the mercury/Tekran site, so we chose the monitor in the same model grid cell (WI site #26).

2.3 Total wet deposition of mercury from EPA MDN

MDN reports total mercury wet deposition since 1995, and as of our analysis operated 110 monitoring sites across the US and Canada, with 31 sites in our defined GLR domain, shown in Fig. 1 (Vermette et al., 1995).

Monthly totals from the Mercury Deposition Network (MDN) were compared to model results by summing CMAQ-Hg values in grid cells containing MDN site according to the MDN start and end times associated with each monitor, rounded to the nearest hour. Monthly totals were calculated using the end date of the MDN measurement period, and MDN reports of zero wet deposition were included. Only in cases where 50 % or more of the reported sampling periods had data missing or invalid from a given MDN monitor, were those sites not counted towards monthly totals.

ACPD
12, 2131–2166, 2012

2.4 Ambient, speciated mercury

As described in Manolopoulos et al. (2007), samples were taken every two hours using a Tekran ambient mercury analyzer (Landis et al., 2002; Lu et al., 1998; Lynam and Keeler, 2002).

The DL site is in a rural area dominated by agriculture, and was collocated with a MDN sampler. The MKE site is an urban setting on the shore of Lake Michigan. While there was no MDN monitor collocated at the site, there was an MDN monitor in the city of Milwaukee, which fell into the same model grid cell as the ambient concentration sampler. Urban emissions around MKE are dominated by a few EGUs; DL has only one EGU and one non-EGU source within 100 km of the measurement site.

3 Model evaluation

3.1 Comparison with ozone, nitrogen dioxide, and sulfur dioxide

To evaluate CMAQ-Hg's ability to capture more commonly simulated atmospheric pollutants, we compare O_3, NO_2, and SO_2 at the DL and MKE study sites in 2003. Daily average measurements were available year-round for O_3 at DL, and for SO_2 at both sites. Ozone at MKE was available during the summer season (15 April to 16 October). Nitrogen dioxide was available at MKE from 23 May onward and at DL from 27 March onward, continuing at both sites through the end of the year. Table 1 provides comparison statistics for all three pollutants at both sites.

We present mean concentrations of O_3, NO_2, and SO_2 in units of parts per billion by volume (ppb), coefficient of determination (R^2), normalized mean bias, and normalized mean error, calculated as follows:

ACPD
12, 2131–2166, 2012

1. Normalized Mean Bias = $\frac{\overline{(D_m - D_o)}}{\overline{D_o}}$

2. Normalized Mean Error = $\frac{\overline{|D_m - D_o|}}{\overline{D_o}}$

where D_m represents the model value and D_o represents the observed value. In the case of O_3, NO_2, and SO_2, mixing ratios (D) are evaluated both as daily means and as monthly means. This allows for more appropriate comparison of mercury errors at DL, where daily mean values may be compared between model and observations for 2003, as well as MKE, where monthly mean values are compared between model (2003) and observation (2004–2005).

Model overall skill is similar for the three pollutants, with the mean error calculated from daily means ranging 34 % for NO_2 at DL to 54 % for SO_2 at MKE. Error in NO_2 and SO_2 is reduced by almost a factor of two when calculated from monthly mean values, reflecting the model's ability to capture seasonal trends in these short-lived pollutants more accurately than day-to-day fluctuations. That both bias and error in O_3 are almost the same, and nearly identical when calculated from daily and monthly values, suggests that model problems in capturing O_3 relate to persistent high biases throughout the year.

For O_3, CMAQ-Hg exhibits a positive bias at both sites, with a normalized mean bias from both daily and monthly means of ∼50 % at MKE and 35 % at DL. Ozone concentrations are similar at the two sites, but the model is able to capture daily fluctuations at the inland, rural DL site more realistically, reflected in a higher R^2 of 0.47, relative to the 0.31 R^2 value at MKE. Previous studies evaluating CMAQ have also found that it captures episodic trends and predicts the daily maximum 8-hour and 1-hour averages relevant to air quality management, but tends to over-predict O_3 values, especially night-time minima (Hogrefe et al., 2011; Mao et al., 2010; Yu et al., 2010).

Ambient concentrations of NO_2 at MKE average about four times higher than those at DL, due to local emissions from transportation, electricity and industry at the urban site.

ACPD
12, 2131–2166, 2012

At DL peak values tend to occur primarily between October and May, when the NO_2 lifetime is long enough to allow transport to the rural site. No obvious NO_2 seasonality is apparent in either the observations or simulation at MKE. CMAQ-Hg tends to under-predict daily NO_2 at both sites, with biases of 16 % at DL and 18 % at MKE, and similar error at both sites (34 % at DL, 37 % at MKE). This performance is comparable to Vijayaraghavan et al. (2009) where CMAQ simulations over the US are also evaluated against AQS measurements, where the model has a negative bias of 15 % and error of 61 %. In our analysis, some of the difference at DL is due to the reporting limit of 2.5 ppb for that monitor, a value reported on 85 days in 2003. Of those 85 days, CMAQ-Hg values were less than 2.5 ppb NO_2 on 71 days. As with O_3, R^2 values for daily NO_2 are significantly higher at DL than at MKE (0.53 vs. 0.18).

Daily average SO_2 averages about 2.5 times higher at MKE than at DL, with a slight positive model bias at MKE. As with NO_2 at DL, the reporting limit for SO_2 impedes a robust model-measurement comparison, as the model simulates values below the apparent reporting limit at both sites (at DL the minimum observed is 1.0 ppb, at MKE, 2.0 ppb). The model overestimates daily SO_2 at the urban site by 17 %, and very slightly underestimates daily SO_2 at the rural site (−3 %), with similar levels of error at both sites (54 % for MKE, 52 % at DL) and similar R^2 values (0.29 for MKE, 0.24 at DL). These comparisons are similar to results in other US studies, which also show a tendency for CMAQ to over-predict SO_2 by 30–50 % (EPA, 2005; Mao et al., 2006).

At the two study sites, as shown in prior model evaluations, CMAQ-Hg does a respectable job at simulating a range of pollutants. Chemical processes and regional transport control modeled O_3, whereas emission patterns and local transport have a greater impact on NO_2 and SO_2. Atmospheric RHg might be expected to perform similarly to NO_2 or SO_2, as a short-lived tracers tied to emission from EGUs. On the other hand, RHg produced from the oxidation of Hg^0 might be expected to perform similarly to O_3, given the important role of this oxidant in the CMAQ-Hg chemical mechanism. In fact, as discussed in Sect. 3.3, below, RHg is significantly overestimated by CMAQ, showing very different behavior than any of these other pollutants.

ACPD
12, 2131–2166, 2012

3.2 Wet deposition

Simulated wet deposition from CMAQ-Hg is compared with observations from the MDN on an annual and seasonal basis in Table 1, where Fig. 1 shows the locations of the GLR measurement sites included in these calculations. For wet deposition R^2, bias, and error, Eqs. (1) and (2), D reflects the annual (or seasonal) mean mercury wet deposition value at each site, so metrics reflect the agreement between model and observations in terms of spatial variability and spatial mean values. On an annual basis, CMAQ-Hg underestimates wet deposition by 21 %, and shows average errors of 55 %. The seasonal low bias ranges from 26–32 % in spring (March, April, May, i.e. MAM), summer (June, July, August, i.e. JJA), and autumn (September, October, November, i.e. SON). However, in winter (December, January, February, i.e. DJF), the model over-predicts total mercury deposition by 70 %. Winter appears to show the worst model performance in general, with errors about twice those of other seasons. Spring shows the lowest model error at 42 %, and the highest R^2 value at 0.54, two to three times higher than any other season.

These results show similar skill to previous studies comparing regional models to MDN results over the US, although biases differ among studies (even studies using CMAQ-Hg), and within single studies among sensitivity tests (Lin et al., 2007; Seigneur et al., 2003a). Depending on the specifics of the simulation, modeled mercury wet deposition has been found to be biased high – e.g. 26 % (spring) and 60 % (summer) (Bullock and Brehme, 2002); 69 % (July) (Bash, 2010); 22 % (annual, higher resolution) (Seigneur et al., 2003a); biased low – e.g. −9 % (annual, lower resolution) (Seigneur et al., 2003a), −11 % (Seigneur et al., 2003b), and others (Cohen et al., 2004; Gbor et al., 2006); and have little bias – e.g. Vijayaraghavan et al. (2008). However, even in cases with low bias, error can still be significant – e.g. 49 % (Vijayaraghavan et al., 2008) and 28–41 % (Seigneur et al., 2003a) comparable to our value of 55 % annual error in the GLR. Values of R^2 emerging from the literature vary widely, and for most time periods our values are in the range of prior estimates. Our annual R^2 value of

ACPD
12, 2131–2166, 2012

0.27 is in the range of 0.14–0.45 (Seigneur et al., 2003a) but lower than 0.72 (Seigneur et al., 2003b). For winter we calculate $R^2 = 0.20$ worse than 0.75–0.91 (Lin et al., 2007), but our spring value of $R^2 = 0.54$ is better than 0.43 (Bullock and Brehme, 2002), and our summer $R^2 = 0.23$, in the range of 0.11 (Bullock and Brehme, 2002), 0.39 (Vijayaraghavan et al., 2008), and 0.59–0.81 (Lin et al., 2007).

These results suggest that our simulated wet deposition reflects the level of agreement with MDN measurements typical among regional models, and with performance only somewhat worse than other simulated species at DL and MKE.

3.3 Ambient mercury concentrations

For consistency with other CMAQ-Hg simulated species, Table 1 includes annual performance metrics for ambient, speciated mercury. Values at DL are calculated from daily mean values, for consistency with the O_3, SO_2, and NO_2 metrics, for all days between 10 April 2003 (start of measurement period) and 31 December 2003 (end of modeling period) in which more than 25 % (6 h) of measurement data were available. Values at both MKE and DL are also calculated from monthly mean values (for months in which more than 25 % of hourly values are recorded). This examination of monthly mean behavior allows for comparison between the May 2004 MKE measurement period and the 2003 modeling period, and reflects model skill in capturing observed seasonal cycles.

Seasonal behavior at the two sites is also apparent in Fig. 2, which compares ambient concentrations at the two sites on a 14-day running average basis. The running average allows us to compare CMAQ-Hg simulations for 2003, with observations from both 2003–2004 (for DL) and 2004–2005 (for MKE). We show here only results from the 12 km × 12 km GLR simulations, and note that differences between the coarser 36 km × 36 km simulation and the finer 12 km × 12 km simulation were not qualitatively significant.

ACPD
12, 2131–2166, 2012

3.3.1 Elemental mercury

Over the April 2003–December 2003 measurement period, Hg^0 at DL averages 1.6 ng m^{-3}, but shows considerable variability on both seasonal and synoptic scales. Average Hg^0 concentrations and variability at DL for Hg^0 are consistent with recent long-term (June 2007–November 2007) observations in rural central Wisconsin using a similar measurement approach (1.3–1.4 ng m^{-3}, Kolker et al., 2010). As shown in Fig. 2, observed summer values regularly dip below 1.5 ng m^{-3} whereas winter concentrations approach 2 ng m^{-3}. Simulated surface concentrations have a similar annual mean values, 1.5 ng m^{-3}, but show significantly less variability than observed. Variability between measurements and models shows almost no correlation either on a daily basis, $R^2 = 0.01$, or on a monthly mean basis, $R^2 = 0.04$. Thus, while mean values agree, and daily mean values reflect low model bias (−6 %) and reasonable error (13 %), model performance with respect to ambient Hg^0 at the rural site does not indicate any particular skill in capturing regional emissions, chemical processes, and/or transport processes. Rather, the model advects boundary values of Hg^0 into the domain, resulting in the adequate simulation of mean values but not observed variability.

As at DL, observed ambient Hg^0 at MKE exhibits much higher variability than do the simulated values, and observations show a significantly higher mean value as well (Fig. 3). Measured annual MKE Hg^0 averages 2.4 ng m^{-3}, with peak values exceeding 4 ng m^{-3}, whereas CMAQ-Hg estimates a value for MKE almost identical to DL at 1.6 ng m^{-3}. This disagreement suggests that elevated urban emissions of Hg^0 and/or reduction of RHg in the urban environment are missing from CMAQ-Hg. Monthly mean values show no correlation between the model and observation ($R^2 = 0.01$, based on monthly mean values), further indicating that processes determining seasonal variability are missing from the model.

Despite the evident shortcomings in CMAQ-Hg's ability to resolve emissions and processes controlling ambient Hg^0, the overall performance statistics are quite good, with normalized biases of −36 % even for MKE, and normalized mean error in the range

ACPD
12, 2131–2166, 2012

(or less than) that seen for any other pollutants considered in Table 1. As in the case of the adequate performance against MDN observations, such good metrics in comparing modeled and observed Hg^0 in prior studies may have suggested unrealistically strong overall model performance.

3.3.2 Reactive mercury

Although CMAQ-Hg performance metrics for wet deposition and ambient Hg^0 are in the range of the more oft-modeled criteria pollutants, performance for reactive mercury species at our two sites is dramatically worse, with annual average biases ranging from 215 % to 331 %. This level of error is five to ten times worse than any of the other annual metrics considered in Table 1, but consistent with the few other studies in which models were evaluated against ambient reactive mercury, noted above in Sect. 1.

That RHg is much too high, whereas wet deposition shows a low bias (and only moderate error) is surprising, given that RHg is the dominant contributor to total mercury wet deposition in our simulations and in past studies (Lin and Tao, 2003). This pattern might be explained by a compensating error in the wet deposition rate, where the deposition rate is too low, balancing the too-high RHg concentrations. An additional hypothesis of too-high dry deposition is explored below. Although speciation between RGHg and PHg represents one source of model error, we find that simulated values of both species are much higher than observed, suggesting that exchange between these two categories would not be expected to improve performance.

At DL, observed RGHg averages 5.4 $pg\,m^{-3}$ and PHg, 8.3 $pg\,m^{-3}$, summing to 14.2 $pg\,m^{-3}$ for RHg over the 2003 monitoring period (Table 1, note that only days where both RGHg and PHg were available are used to calculate RHg); both species are higher at DL than median values of 0.6–0.8 $pg\,m^{-3}$ (RGHg) and 2.6–5.0 $pg\,m^{-3}$ (PHg) reported at nearby sites for the June 2007–November 2007 period (Kolker et al., 2010). CMAQ-Hg averages over three times higher than observations over the 2003 simulation period, with simulated RGHg at 22.6 $pg\,m^{-3}$, PHg at 29.2 $pg\,m^{-3}$, and RHg at 52.6 $pg\,m^{-3}$. Neither RGHg nor PHg show agreement in variability between

ACPD
12, 2131–2166, 2012

simulated and observed values, with daily R^2 values of 0.04 and 0.05 respectively. Interestingly, the daily R^2 of RHg (0.10) is twice as high as either RGHg or PHg, suggesting that the allocation of the reactive forms is a source of error, even if not the dominant source of error. Model performance is especially bad in summer months at DL, as shown in Fig. 2. In August, CMAQ-Hg overestimates RGHg by a factor of about 15 relative to observed values, and overestimates PHg by a factor of 5.

Only in April 2003 does RGHg show relative agreement between model and observations at DL (Fig. 2). At the rural site, local emissions are effectively zero, and measured RHg may be attributed to transport or to local chemical production. Observed RHg concentrations at DL were highest in April and the first half of May, and wind direction measurements taken at the site show that winds were predominantly easterly during that time, compared to prevailing westerly winds the rest of the year (Fig. 4). During the easterly wind events, the DL measured RHg concentrations show a significant increase, most likely reflecting advection from high-emitting areas to the east (Milwaukee area) (Rutter et al., 2008a). Both observed and modeled winds show advection from the east in April and early May, versus from the west/southwest in June–December.

While CMAQ-Hg shows similar wind patterns to observations (Fig. 4) and a similar eastward concentration gradient in RGHg (Table 1), the model does not yield the higher springtime RGHg surface concentrations at DL seen in the observations (Fig. 2b). This evidence points to a modeled RGHg lifetime in CMAQ-Hg that is too short, impeding the transport of emitted RGHg to DL in Spring 2003. Because RGHg lifetime is strongly dependent on dry deposition, we hypothesize that dry deposition rates are unrealistically high in the model.

As at DL, CMAQ-Hg significantly over-predicts RHg concentrations at MKE, with mean biases in RGHg of 331 % and PHg of 215 %. Relative to DL, the model is better able to capture the seasonal cycle (variability of monthly means) at MKE, with R^2 values of 0.24 for RGHg and 0.11 for PHg (Table 1, Fig. 3).

We can also evaluate the urban-rural differences between modeled and observed values. Both measurements and model suggest that annual RHg is about 50 % higher

ACPD
12, 2131–2166, 2012

at MKE that at DL. However, the allocation between RGHg and PHg differs, with measurements showing with PHg is about 50 % higher than RGHg at the rural site, and about 20 % higher at the urban site, where the model shows less of a difference at the rural site (30 %) and the opposite pattern (higher RGHg) a the urban site.

Overall, RHg in CMAQ-Hg shows biases, error, and lack of correlation with observations far worse than other mercury metrics (Hg^0 and wet deposition) and other pollutants (O_3, NO_2, and SO_2). Below, we consider sources of these errors by isolating mercury sources from within the domain vs. long-range transport.

3.4 Regional emissions vs. long-range transport

The major over-prediction of RHg at both DL and MKE, especially in concert with the under-prediction of wet deposition relative to MDN measurements, raises questions about model processes, including emissions, model chemistry and/or removal processes.

To identify how emissions and chemistry each contribute to the budget of RHg, we conducted a sensitivity simulation to isolate the impacts of background mercury on the DL and MKE study sites. Here we define "background" as import to the GLR from the broader CONUS domain, which in turn includes global import via fixed boundary values (Table A1). A "zero background" (ZB) scenario was run, with no mercury species advecting into the GLR for July 2003 (including a 10-day spin-up period). All other boundary conditions between the CONUS and GLR domains were unaltered. The results from the ZB run reflect the impacts of emissions alone for the GLR. Subtracting these results from the base case (BC) results discussed above yields an estimate of mercury associated with background only – i.e. "zero emissions" (ZE). We compare the ZB and ZE results to quantify relative influence of local emissions versus imported mercury and precursors, and how these results compare to observations.

Figure 5 (DL) and Fig. 6 (MKE) compare concentrations for Hg^0 (Figs. 5a, 6a) and RHg (Figs. 5b, 6b) over July 2003 between measurements and simulated concentrations (BC, ZB, ZE = BC-ZB). Metrics for the comparisons among the simulations are

ACPD
12, 2131–2166, 2012

presented in Table 2, calculated from daily averaged values at DL and monthly mean values from MKE.

At DL, the CMAQ-Hg BC results are very similar to the ZE case, suggesting that boundary inflow alone contributes the majority of simulated mercury at the rural site, in both elemental and reactive forms. 99 % of the BC-simulated Hg^0 is captured by the ZE scenario, and 91 % of BC-simulated RHg is captured. This attribution directly informs the errors discussed above, in that the major over-prediction of ground-level RHg at DL appears to be due to errors in chemistry and/or deposition affecting boundary inflow. Removing all inflow of mercury (ZB) leads to significantly improved model performance for RHg, with the normalized mean error dropping from 483 % to 68 %.

The lower error and −44 % bias associated with the ZB case at DL still points to major model problems, especially in light of the extremely low R^2 value of 0.01, suggesting no relationship between variability in observed and modeled RHg. Thus, removing boundary inflow cannot be considered an option to "fix" the extreme high model bias, but rather it suggests that erroneous processing of boundary inflow combines with additional errors (especially with respect to regional emissions) to create the erroneous estimate of ambient RHg.

At MKE, we again compare measurements from July 2004 with model results from July 2003. As at DL, ambient Hg^0 values are near-zero when boundary inflow is removed (ZB). There is a clear difference, however, in the response of modeled RHg to the removal of inflow at the urban and rural sites. Whereas 91 % of DL RHg is captured by the ZE scenario, at MKE only 55 % of RHg is attributable to boundary inflow. The sensitivity of RHg at DL vs. MKE to the removal of boundary inflow indicates that local emissions are having an impact on simulated RHg at the urban site, but that the atmospheric lifetime of these RHg emissions is not long enough in the model to promote transport to DL. This behavior is further evidence, along with the model's inability to capture observed April peaks in RHg at DL, of too-high dry deposition rates in CMAQ-Hg.

ACPD
12, 2131–2166, 2012

4 Discussion

The comparison of CMAQ-Hg performance with observations at a rural and urban site suggests that the model contains a number of significant errors in the treatment of atmospheric mercury. These errors have not been clear in past studies comparing with total mercury wet deposition, ambient Hg^0, and ambient total gaseous mercury (TGM), given the role of boundary conditions in determining Hg^0 and TGM, and potentially compensating errors in determining total wet deposition.

Based on our analysis, we suggest that production of RHg from Hg^0 is too high in the model, emissions of RHg and Hg^0 in urban areas are incorrect, mercury wet deposition rates are too low, and mercury dry deposition rates are too high. As a result of these errors, directly emitted RHg exhibits an unrealistically short lifetime in CMAQ-Hg, and boundary inflow contributes too much to surface RHg and wet deposition.

Together, these errors suggest that CMAQ-Hg underestimates the degree to which regional emissions contribute to wet deposition, and overestimates the contribution of international sources to US mercury deposition. The finding that long-range transport of mercury dominates wet deposition has been advanced by global modeling studies suggesting that only 20–30 % of total US deposition is attributable North American anthropogenic emissions (Seigneur et al., 2004; Selin and Jacob, 2008), and a regional modeling study over Asia also attributes 30 % of total deposition to regional emissions (Pan et al., 2010). The degree to which these important estimates are valid depends critically on each model's ability to capture key processes controlling mercury deposition. Given the dominant contribution of Hg^0 to total atmospheric mercury, even small changes in reaction rates, chemical cycling, and deposition could have a pronounced impact on source attribution.

The operationally defined nature of the current measurement methods means that there may be some oxidized mercury species which are not included in the model but which were collected and measured. For example, recent model and observational studies have suggested that the bromine oxidation pathway may be important in

ACPD
12, 2131–2166, 2012

the mid-latitudes, and therefore also the product, $HgBr_2$ (Holmes et al., 2010; Obrist et al., 2011). In contrast, some species may be collected and measured by the instrument with less than 100 % efficiency, but which are included in the model without accounting for this. Recent publications have provided empirical evidence suggesting that the Tekran Ambient Mercury Analyzer may be subject to measurement artifacts diminishing collection efficiencies: Lyman et al. (2010) show that RGM may be undermeasured during high ozone events, while Rutter et al. (2008b) and Talbot et al. (2011) both suggest that PHg detected on filters was lost and not measured, probably due to the instrument being heated to 50 °C rather than being held at ambient temperature. However, the discrepancies between observations and model outputs observed in this study cannot be explained by any of the differences in measurement efficiency, or by how CMAQ-Hg converts between chemical species and operationally defined species.

5 Conclusions

Our choice of CMAQ-Hg as an analysis tool was motivated by its strong track record of development and analysis, and good performance against available measurements from the US EPA MDN. In embarking on this study, we hoped to find the model reasonable in its ambient concentration estimates, and relevant for further scientific experimentation. Unfortunately, our evaluation uncovered fundamental errors in modeled ambient concentrations, traced back to likely errors in chemistry, deposition, and emissions.

Like other studies, we find reasonable agreement between model estimates of total wet deposition and those measured by the MDN. However, the favorable agreement appears to be due to compensating errors, in light of the over-prediction of surface RHg concentration and potential under-prediction of RHg lifetime and/or under-prediction of wet deposition rates. In this sense, the chemical processes for atmospheric mercury remain uncertain and advanced research into the chemical kinetics would aid modeling efforts and characterization of even basic source-receptor questions.

ACPD
12, 2131–2166, 2012

Acknowledgements. This work was supported by EPA STAR Grant R833375, with SNS supported by EPA STAR Grant R831840. Thanks to Erica Scotty for assistance with data processing.

References

Bash, J. O.: Description and initial simulation of a dynamic bidirectional air-surface exchange model for mercury in Community Multiscale Air Quality (CMAQ) model, J. Geophys. Res., 115, 1–15, doi:10.1029/2009JD012834, 2010.

Binkowski, F. S. and Roselle, S. J.: Models-3 Community Multiscale Air Quality (CMAQ) model aerosol component 1. Model description, J. Geophys. Res., 108, 4183, doi:10.1029/2001JD001409, 2003.

Binkowski, F. S. and Shankar, U.: The Regional Particulate Matter Model 1. Model description and preliminary results, J. Geophys. Res., 100, 26191–26209, 1995.

Bullock Jr., O. R. and Braverman, T.: Application of the CMAQ mercury model for US EPA regulatory support, Developments in Environmental Sciences, 6, 85–95, doi:10.1016/S1474-8177(07)06022-6, 2007.

Bullock Jr., O. R. and Brehme, K. A.: Atmospheric mercury simulation using the CMAQ model: formulation description and analysis of wet deposition results, Atmos. Environ., 36, 2135–2146, doi:10.1016/S1352-2310(02)00220-0, 2002.

Bullock Jr., O. R., Atkinson, D., Braverman, T., Civerolo, K., Dastoor, A., Davignon, D., Ku, J.-Y., Lohman, K., Myers, T. C., Park, R. J., Seigneur, C., Selin, N. E., Sistla, G., and Vijayaraghavan, K.: An analysis of simulated wet deposition of mercury from the North American Mercury Model Intercomparison Study, J. Geophys. Res., 114, 1–12, doi:10.1029/2008JD011224, 2009.

Byun, D. and Schere, K. L.: Review of the Governing Equations, Computational Algorithms, and Other Components of the Models-3 Community Multiscale Air Quality (CMAQ) Modeling System, Appl. Mech. Rev., 59, 51, doi:10.1115/1.2128636, 2006.

Cohen, M., Artz, R., Draxler, R., Miller, P., Poissant, L., Niemi, D., Ratte, D., Deslauriers, M., Duval, R., Laurin, R., Slotnick, J., Nettesheim, T., and McDonald, J.: Modeling the atmospheric transport and deposition of mercury to the Great Lakes, Environ. Res., 95, 247–265, doi:10.1016/j.envres.2003.11.007, 2004.

ACPD

12, 2131–2166, 2012

EPA: CMAQ Model Performance Evaluation for 2001: Updated March 2005, US Environmental Protection Agency Report, (March), 2005.

Gbor, P., Wen, D., Meng, F., Yang, F., Zhang, B., and Sloan, J.: Improved model for mercury emission, transport and deposition, Atmos. Environ., 40, 973–983, doi:10.1016/j.atmosenv.2005.10.040, 2006.

Gbor, P., Wen, D., Meng, F., Yang, F., and Sloan, J.: Modeling of mercury emission, transport and deposition in North America, Atmos. Environ., 41, 1135–1149, doi:10.1016/j.atmosenv.2006.10.005, 2007.

Gery, M. W., Whitten, G. Z., Killus, J. P., and Dodge, M. C.: A Photochemical Kinetics Mechanism for Urban and Regional Scale Computer Modeling, J. Geophys. Res., 94, 12925–12956, 1989.

Hogrefe, C., Hao, W., Zalewsky, E. E., Ku, J.-Y., Lynn, B., Rosenzweig, C., Schultz, M. G., Rast, S., Newchurch, M. J., Wang, L., Kinney, P. L., and Sistla, G.: An analysis of long-term regional-scale ozone simulations over the Northeastern United States: variability and trends, Atmos. Chem. Phys., 11, 567–582, doi:10.5194/acp-11-567-2011, 2011.

Holmes, C. D., Jacob, D. J., Corbitt, E. S., Mao, J., Yang, X., Talbot, R., and Slemr, F.: Global atmospheric model for mercury including oxidation by bromine atoms, Atmos. Chem. Phys., 10, 12037–12057, doi:10.5194/acp-10-12037-2010, 2010.

Kolker, A., Olson, M. L., Krabbenhoft, D. P., Tate, M. T., and Engle, M. A.: Patterns of mercury dispersion from local and regional emission sources, rural Central Wisconsin, USA, Atmos. Chem. Phys., 10, 4467–4476, doi:10.5194/acp-10-4467-2010, 2010.

Landis, M. S., Vette, A. F., and Keeler, G. J.: Atmospheric mercury in the Lake Michigan basin: influence of the Chicago/Gary urban area, Environ. Sci. Technol., 36, 4508–4517, 2002.

Lin, C., and Pehkonen, S. O.: The chemistry of atmospheric mercury: a review, Atmos. Environ., 33, 2067–2079, doi:10.1016/S1352-2310(98)00387-2, 1999.

Lin, C.-J., Pongprueksa, P., Lindberg, S. E., Pehkonen, S. O., Byun, D., and Jang, C.: Scientific uncertainties in atmospheric mercury models I: Model science evaluation, Atmos. Environ., 40, 2911–2928, doi:10.1016/j.atmosenv.2006.01.009, 2006.

Lin, C.-J., Pongprueksa, P., Russell Bullock Jr., O., Lindberg, S. E., Pehkonen, S. O., Jang, C., Braverman, T., and Ho, T. C.: Scientific uncertainties in atmospheric mercury models II: Sensitivity analysis in the CONUS domain, Atmos. Environ., 41, 6544–6560, doi:10.1016/j.atmosenv.2007.04.030, 2007.

Lin, X. and Tao, Y.: A numerical modelling study on regional mercury budget for eastern North

ACPD
12, 2131–2166, 2012

America, Atmos. Chem. Phys., 3, 535–548, doi:10.5194/acp-3-535-2003, 2003.
Lindberg, S., Bullock, O. R., Ebinghaus, R., Engstrom, D., Feng, X., Fitzgerald, W., Pirrone, N., Prestbo, E., and Seigneur, C.: A synthesis of progress and uncertainties in attributing the sources of mercury in deposition., Ambio, 36, 19–32, 2007.
Lohman, K., Seigneur, C., Edgerton, E., and Jansen, J.: Modeling mercury in power plant plumes., Environ. Sci. Technol., 40, 3848–3854, 2006.
Lohman, K., Seigneur, C., Gustin, M., and Lindberg, S.: Sensitivity of the global atmospheric cycle of mercury to emissions, Appl. Geochem., 23, 454–466, doi:10.1016/j.apgeochem.2007.12.022, 2008.
Lu, J. Y., Schroeder, W. H., Berg, T., Munthe, J., Schneeberger, D., and Schaedlich, F.: A device for sampling and determination of total particulate mercury in ambient air, Anal. Chem., 70, 2403–2408, doi:10.1021/ac971278l, 1998.
Lyman, S. N., Jaffe, D. A., and Gustin, M. S.: Release of mercury halides from KCl denuders in the presence of ozone, Atmos. Chem. Phys., 10, 8197–8204, doi:10.5194/acp-10-8197-2010, 2010.
Lynam, M. M. and Keeler, G. J.: Comparison of methods for particulate phase mercury analysis: sampling and analysis, Anal. Bioanal. Chem., 374, 1009–1014, doi:10.1007/s00216-002-1584-4, 2002.
Manolopoulos, H., Schauer, J. J., Purcell, M. D., Rudolph, T. M., Olson, M. L., Rodger, B., and Krabbenhoft, D. P.: Local and regional factors affecting atmospheric mercury speciation at a remote location, Journal of Environmental Engineering and Science, 6, 491–501, doi:10.1139/S07-005, 2007.
Mao, H., Chen, M., Hegarty, J. D., Talbot, R. W., Koermer, J. P., Thompson, A. M., and Avery, M. A.: A comprehensive evaluation of seasonal simulations of ozone in the northeastern US during summers of 2001–2005, Atmos. Chem. Phys., 10, 9–27, doi:10.5194/acp-10-9-2010, 2010.
Mao, Q., Gautney, L., Cook, T., Jacobs, M., Smith, S., and Kelsoe, J.: Numerical experiments on MM5–CMAQ sensitivity to various PBL schemes, Atmos. Environ., 40, 3092–3110, doi:10.1016/j.atmosenv.2005.12.055, 2006.
Mesinger, F., DiMego, G., Kalnay, E., Mitchell, K., Shafran, P. C., Ebisuzaki, W., Jović, D., Woollen, J., Rogers, E., Berbery, E. H., Ek, M. B., Fan, Y., Grumbine, R., Higgins, W., Li, H., Lin, Y., Manikin, G., Parrish, D., and Shi, W.: North American Regional Reanalysis, B. Am. Meteorol. Soc., 87, 343–360, doi:10.1175/BAMS-87-3-343, 2006.

ACPD
12, 2131–2166, 2012

Obrist, D., Tas, E., Peleg, M., Matveev, V., Fain, X., Asaf, D., and Luria, M.: Bromine-induced oxidation of mercury in the mid-latitude atmosphere, Nature Geosci., 4, 22–26, doi:10.1038/ngeo1018, 2011.

Pan, L., Lin, C.-J., Carmichael, G. R., Streets, D. G., Tang, Y., Woo, J.-H., Shetty, S. K., Chu, H.-W., Ho, T. C., Friedli, H. R., and Feng, X.: Study of atmospheric mercury budget in East Asia using STEM-Hg modeling system, Sci. Total Environ., 408, 3277–3291, doi:10.1016/j.scitotenv.2010.04.039, 2010.

Pleim, J. E., Finkelstein, P. L., Clarke, J. F., and Ellestad, T. G.: A technique for estimating dry deposition velocities based on similarity with latent heat flux, Atmos. Environ., 33, 2257–2268, doi:10.1016/S1352-2310(98)00162-9, 1999.

Rutter, A. P., Schauer, J. J., Lough, G. C., Snyder, D. C., Kolb, C. J., Von Klooster, S., Rudolf, T., Manolopoulos, H., and Olson, M. L.: A comparison of speciated atmospheric mercury at an urban center and an upwind rural location., J. Environ. Monit., 10, 102–108, doi:10.1039/b710247j, 2008a.

Rutter, A. P., Hanford, K. L., Zwers, J. T., Perillo-Nicholas, A. L., Schauer, J. J., Worley, C. A., Olson, M. L., and DeWild, J. F.: Evaluation of an off-line method for the analysis of atmospheric reactive gaseous mercury and particulate mercury, J. Air Waste Manage. Assoc., 58, 377–383, 2008b.

Sanei, H., Outridge, P. M., Goodarzi, F., Wang, F., Armstrong, D., Warren, K., and Fishback, L.: Wet deposition mercury fluxes in the Canadian sub-Arctic and southern Alberta, measured using an automated precipitation collector adapted to cold regions, Atmos. Environ., 44, 1672–1681, doi:10.1016/j.atmosenv.2010.01.030, 2010.

Sarwar, G., Luecken, D., Yarwood, G., Whitten, G. Z., and Carter, W. P. L.: Impact of an Updated Carbon Bond Mechanism on Predictions from the CMAQ Modeling System: Preliminary Assessment, J. Appl. Meteorol. Climatol., 47, 3–14, doi:10.1175/2007JAMC1393.1, 2008.

Seigneur, C., Karamchandani, P., Vijayaraghavan, K., and Lohman, K.: On the effect of spatial resolution on atmospheric mercury modeling, Environment, 304, 73–81, 2003a.

Seigneur, C., Lohman, K., Vijayaraghavan, K., and Shia, R.-L.: Contributions of global and regional sources to mercury deposition in New York State, Environ. Pollut., 123, 365–373, doi:10.1016/S0269-7491(03)00027-7, 2003b.

Seigneur, C., Vijayaraghavan, K., Lohman, K., Karamchandani, P., and Scott, C.: Global source attribution for mercury deposition in the United States, Environ. Sci. Technol., 38, 555–569, 2004.

ACPD
12, 2131–2166, 2012

Selin, N. E.: Global Biogeochemical Cycling of Mercury: A Review, Annu. Rev. Environ. Res., 34, 43–63, doi:10.1146/annurev.environ.051308.084314, 2009.
Selin, N. E., Jacob, D. J., Park, R. J., Yantosca, R. M., Strode, S., Jaeglé, L., and Jaffe, D.: Chemical cycling and deposition of atmospheric mercury: Global constraints from observations, J. Geophys. Res., 112, 1–14, doi:10.1029/2006JD007450, 2007.
Selin, N. E. and Jacob, D. J.: Seasonal and spatial patterns of mercury wet deposition in the United States: Constraints on the contribution from North American anthropogenic sources, Atmos. Environ., 42, 5193–5204, doi:10.1016/j.atmosenv.2008.02.069, 2008.
Skamarock, W. and Klemp, J.: A time-split nonhydrostatic atmospheric model for weather research and forecasting applications, J. Comput. Phys., 227, 3465–3485, doi:10.1016/j.jcp.2007.01.037, 2008.
Soerensen, A. L., Sunderland, E. M., Holmes, C. D., Jacob, D. J., Yantosca, R. M., Skov, H., Christensen, J. H., Strode, S. A., and Mason, R. P.: An improved global model for air-sea exchange of mercury: high concentrations over the North Atlantic., Environ. Sci. Technol., 44, 8574–8580, doi:10.1021/es102032g, 2010.
Talbot, R., Mao, H., Feddersen, D., Smith, M., Kim, S. Y., Sive, B., Haase, K., Ambrose, J., Zhou, Y., and Russo, R.: Comparison of Particulate Mercury Measured with Manual and Automated Methods, Atmosphere, 2, 1–20, doi:10.3390/atmos2010001, 2011.
Toole-O'Neil, B., Tewalt, S. J., Finkelman, R. B., and Akers, D. J.: Mercury concentration in coal—unraveling the puzzle, Fuel, 78, 47–54, doi:10.1016/S0016-2361(98)00112-4, 1999.
Vermette, S., Lindberg, S., and Bloom, N.: Field tests for a regional mercury deposition network–sampling design and preliminary test results, Atmos. Environ., 29, 1247–1251, doi:10.1016/1352-2310(94)00321-B, 1995.
Vijayaraghavan, K., Karamchandani, P., Seigneur, C., Balmori, R., and Chen, S.-Y.: Plume-in-grid modeling of atmospheric mercury, J. Geophys. Res., 113, 1–12, doi:10.1029/2008JD010580, 2008.
Vijayaraghavan, K., Seigneur, C., Karamchandani, P., and Chen, S.-Y.: Development and Application of a Multipollutant Model for Atmospheric Mercury Deposition, J. Appl. Meteorol. Climatol., 46, 1341–1353, doi:10.1175/JAM2536.1, 2007.
Vijayaraghavan, K., Zhang, Y., Seigneur, C., Karamchandani, P., and Snell, H. E.: Export of reactive nitrogen from coal-fired power plants in the U.S.: Estimates from a plume-in-grid modeling study, J. Geophys. Res., 114, 1–11, doi:10.1029/2008JD010432, 2009.
Wen, D., Lin, J. C., Meng, F., Gbor, P. K., He, Z., and Sloan, J. J.: Quantitative assessment

ACPD
12, 2131–2166, 2012

of upstream source influences on total gaseous mercury observations in Ontario, Canada, Atmos. Chem. Phys., 11, 1405–1415, doi:10.5194/acp-11-1405-2011, 2011.

Yu, S., Mathur, R., Sarwar, G., Kang, D., Tong, D., Pouliot, G., and Pleim, J.: Eta-CMAQ air quality forecasts for O_3 and related species using three different photochemical mechanisms (CB4, CB05, SAPRC-99): comparisons with measurements during the 2004 ICARTT study, Atmos. Chem. Phys., 10, 3001–3025, doi:10.5194/acp-10-3001-2010, 2010.

ACPD

12, 2131–2166, 2012

Table 1. Mean values and evaluation metrics are presented to compare CMAQ-Hg with available measurements of O_3, NO_2, and SO_2 (at DL and MKE, units ppbv); mercury wet deposition across the GLR region (units ng m^{-2}); and Hg^0 (units ng m^{-3}), RGHg, PHg, and RHg (= RGHg + PHg, units pg m^{-3}) at DL and MKE. Equations (1) and (2) used to calculate normalized mean bias and error. All model and measurement data from 2003, except for ambient mercury species at MKE, as discussed in the text.

	CMAQ	Obs	R^2	Norm. Mean Bias (%)	Norm. Mean Error (%)
O_3 mixing ratio (ppb)					
DL Daily means	44	33	0.47	35	37
Monthly means	”	”	0.88	35	35
MKE Daily means	45	30	0.31	50	53
Monthly means	44	29	0.68	52	52
NO_2 mixing ratio (ppb)					
DL Daily means	3.2	3.8	0.53	−16	34
Monthly means	3.2	3.9	0.87	−19	22
MKE Daily means	14	17	0.18	−18	37
Monthly means	14	16	0.13	−14	20
SO_2 mixing ratio (ppb)					
DL Daily means	1.5	1.5	0.24	−3	52
Monthly means	”	”	0.52	0	18
MKE Daily means	3.8	3.3	0.29	17	54
”Monthly means		”	0.47	17	27
Mercury Wet Deposition (ng m^{-2})					
MDN sites	580.4	738.7	0.27	−21	55
Winter (DJF)	373.4	219.6	0.20	70	97
Spring (MAM)	560.7	780.4	0.54	−28	42
Summer (JJA)	890.7	1304.5	0.23	−32	52
Fall (SON)	522.5	704.2	0.13	−26	60

ACPD
12, 2131–2166, 2012

Table 1. Continued.

	CMAQ	Obs	R^2	Norm. Mean Bias (%)	Norm. Mean Error (%)
Hg^0 (ng m^{-3})					
DL Daily means	1.5	1.6	0.01	−6	13
Monthly means	1.5	1.6	0.04	−6	10
MKE Monthly means	1.6	2.4	0.01	−36	36
RGHg (pg m^{-3})					
DL Daily means	22.6	5.4	0.04	318	329
Monthly means	22.6	5.4	0.02	299	299
MKE Monthly means	40.7	9.4	0.24	331	331
PHg (pg m^{-3})					
DL Daily means	29.2	8.3	0.05	254	259
Monthly means	29.2	8.3	0.00	259	259
MKE *(monthly; see caption)*	36.2	11.5	0.11	215	215
RHg (pg m^{-3})					
DL Daily means	52.6	14.2	0.10	269	269
Monthly means	52.6	14.2	0.01	261	261
MKE *(monthly; see caption)*	76.9	21.4	0.07	260	260

ACPD
12, 2131–2166, 2012

Table 2. Mean values and evaluation metrics are presented to compare sensitivity simulations – BC, ZB, and ZE – of CMAQ-Hg with available measurements of Hg^0 (units ng m^{-3}), RGHg, PHg, and RHg (= RGHg + PHg, units pg m^{-3}) at DL and MKE. Equations (1) and (2) used to calculate normalized mean bias and error. All model and DL measurement data from July 2003; measurement data at MKE from July 2004.

	CMAQ	Obs	R^2	Norm. Mean Bias (%)	Norm. Mean Error (%)
DL – Devils Lake, July 2003 Daily Values Hg^0 (ng m^{-3})					
BC	1.46	1.53	0.28	−3	9
ZB	0.02	–	0.00	−98	98
ZE	1.44	–	0.26	−5	10
RHg (pg m^{-3})					
BC	60.88	10.42	0.00	459	460
ZB	5.44	–	0.00	−49	61
ZE	55.43	–	0.00	409	409
MKE – Milwaukee, July 2003 Hg^0 (ng m^{-3})					
BC	1.5	2.1	–	–	–
ZB	0.1	–	–	–	–
ZE	1.4	–	–	–	–
RHg (pg m^{-3})					
BC	97.7	17.3	–	–	–
ZB	43.8	–	–	–	–
ZE	53.9	–	–	–	–

ACPD
12, 2131–2166, 2012

Table A1. Boundary and initial condition values used in CMAQ-Hg for CONUS domain simulation; GLR simulation, which is the basis of all data presented in the text, used boundary values from the CONUS domain.

	Sigma (σ) layer range					
Species	1.00–0.98	0.98–0.93	0.93–0.84	0.84–0.60	0.60–0.30	0.30.0.00
Hg^0 (ppm)	1.780×10^{-7}	1.770×10^{-7}	1.760×10^{-7}	1.750×10^{-7}	1.740×10^{-7}	1.730×10^{-7}
RGHg (ppm)	2.000×10^{-9}	3.000×10^{-9}	4.000×10^{-9}	5.000×10^{-9}	62.000×10^{-9}	7.000×10^{-9}
PHg (ug m^{-3})	1.080×10^{-5}	1.026×10^{-5}	9.718×10^{-6}	7.558×10^{-6}	4.859×10^{-6}	1.620×10^{-6}
Only j-mode						

ACPD
12, 2131–2166, 2012

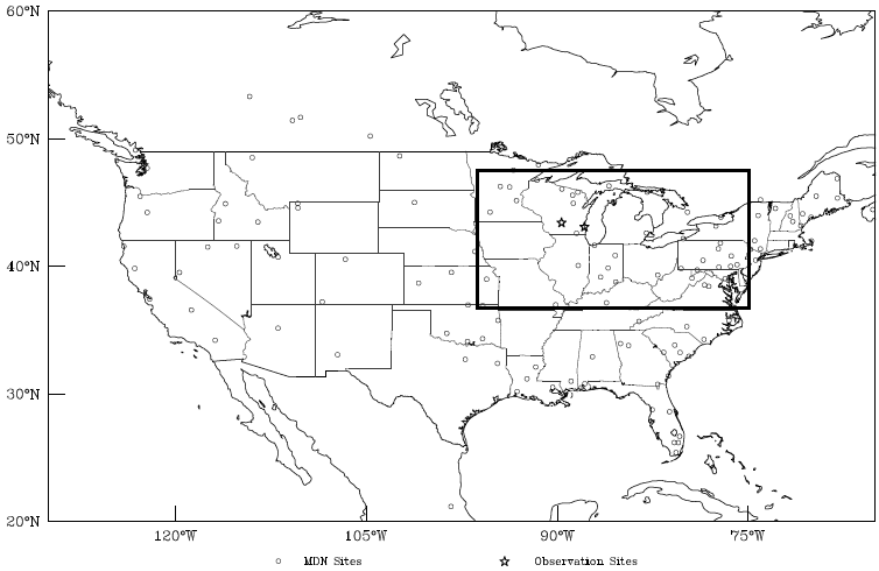

Fig. 1. Domains used for CMAQ-Hg simulations: large box shows the CONUS domain, small box shows the GLR domain. Open circles show locations of MDN monitoring sites; those within the smaller box were analyzed in Table 1. Stars show locations of DL and MKE monitoring sites.

ACPD
12, 2131–2166, 2012

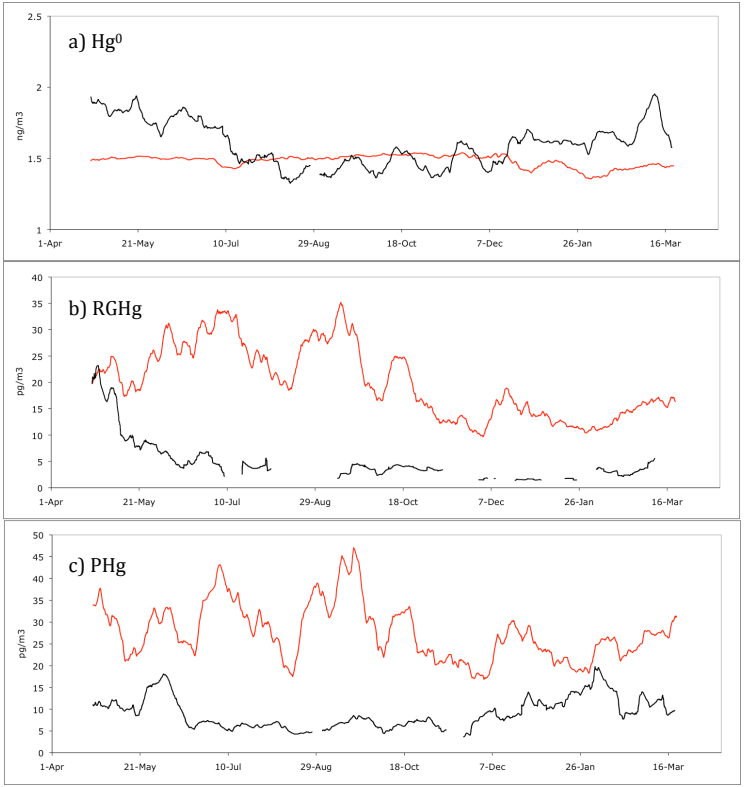

Fig. 2. Comparison of CMAQ-Hg simulated ambient mercury species against observed values at the rural DL site for Hg^0 (**a**, units ng m^{-3}), RGHg (**b**, units pg m^{-3}), and PHg (**c**, units pg m^{-3}). Values reflect a 14-day running average. Observed data spans 2003–2004; model data taken from a 2003 annual simulation.

ACPD
12, 2131–2166, 2012

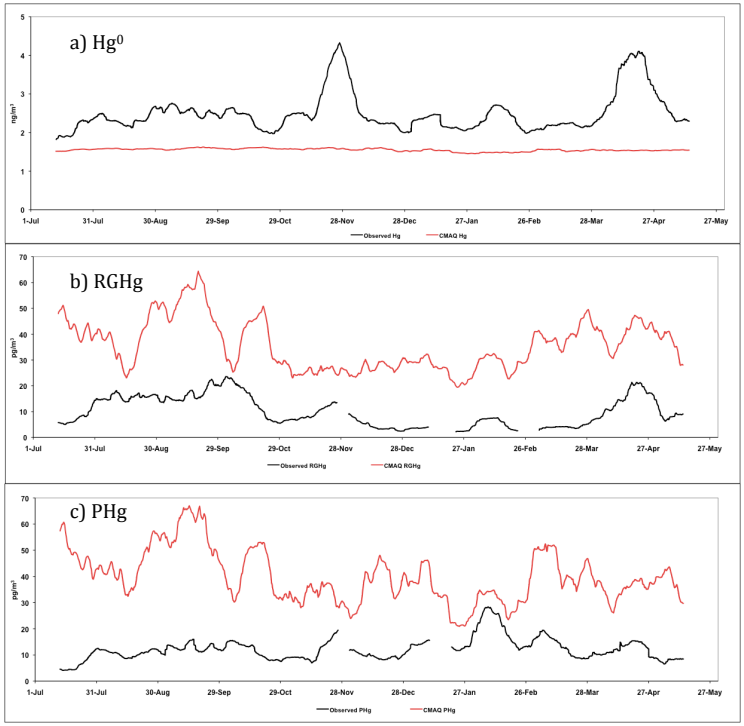

Fig. 3. Comparison of CMAQ-Hg simulated ambient mercury species against observed values at the urban MKE site for Hg^0 (**a**, units ng m^{-3}), RGHg (**a**, units pg m^{-3}), and PHg (**a**, units pg m^{-3}). Values reflect a 14-day running average. Observed data spans 2004–2005; model data taken from a 2003 annual simulation.

ACPD
12, 2131–2166, 2012

a) Observed

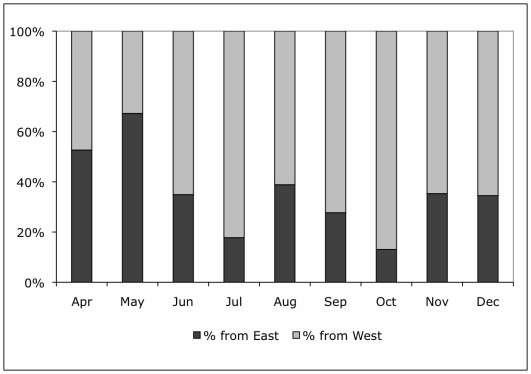

b) Modeled

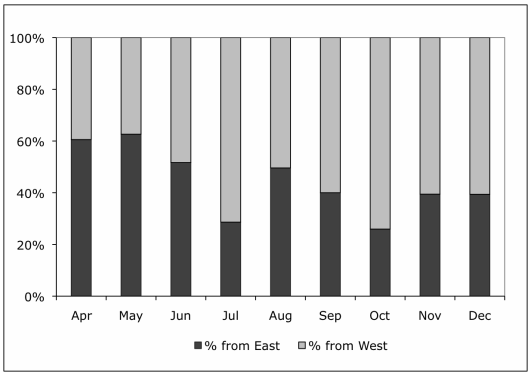

Fig. 4. 2003 wind direction at DL from **(a)** measurements (Rutter et al., 2008a); **(b)** CMAQ-Hg (10-meter wind-speed generated by the WRF model and processed with MCIP v. 3.4). Wind direction was aggregated such that all directions between 0° and 179° were considered from the east and all wind directions greater than or equal to 180° were labeled as from the west.

ACPD
12, 2131–2166, 2012

Fig. 5. Comparison of July 2003 CMAQ-Hg simulated ambient mercury species at DL in the base case (BC), zero boundary inflow (ZB), and zero emissions (ZE) cases against observed values for Hg^0 (**a**, units ng m^{-3}) and RHg (**b**, units pg m^{-3}).

ACPD
12, 2131–2166, 2012

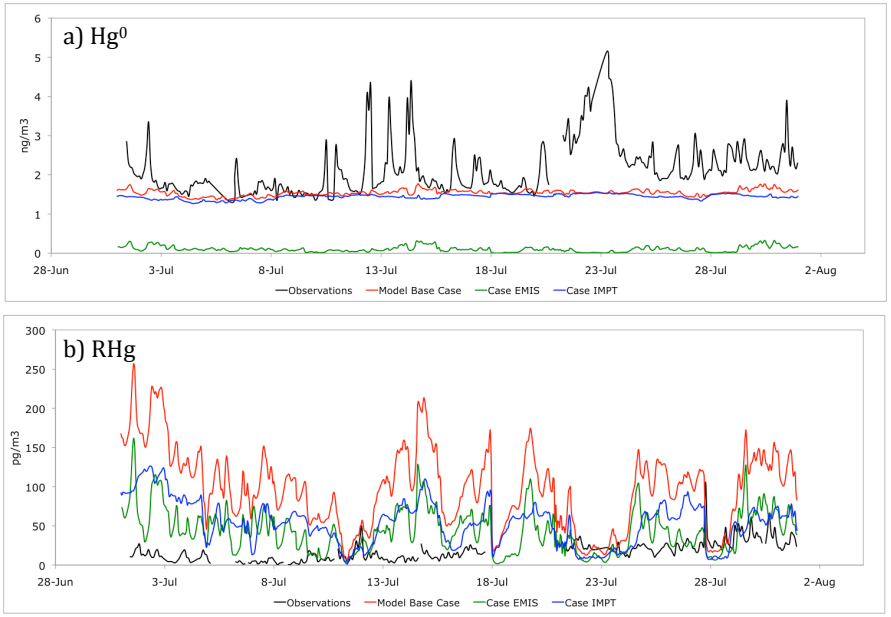

Fig. 6. Comparison of July 2003 CMAQ-Hg simulated ambient mercury species at MKE in the base case (BC), zero boundary inflow (ZB), and zero emissions (ZE) cases against July 2004 observed values for Hg^0 (**a**, units ng m^{-3}) and RHg (**b**, units pg m^{-3}).

ACPD
12, 2131–2166, 2012

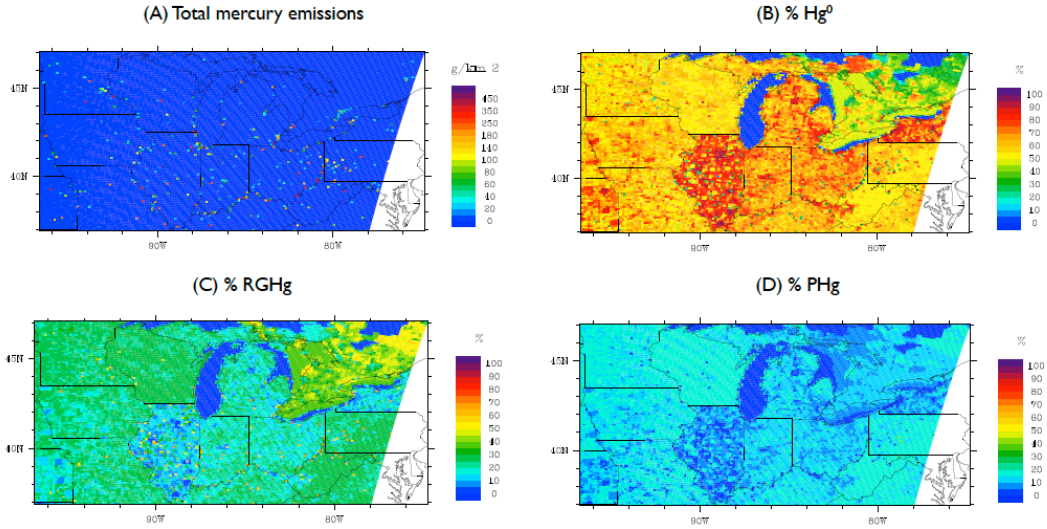

Fig. A1. Mercury emissions used in CMAQ-Hg, taken from the 2002 EPA National Emissions Inventory (NEI) and processed through the SMOKE model. Total mercury emissions **(a)** are given in g km^{-2}, as well as percent (%) allocation to Hg^0 **(b)**, RGHg **(c)** and PHg **(d)**.

ACPD
12, 2131–2166, 2012